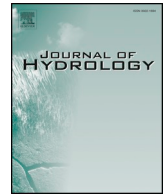




ELSEVIER

Contents lists available at ScienceDirect

Journal of Hydrology

journal homepage: [www.elsevier.com/locate/jhydrol](http://www.elsevier.com/locate/jhydrol)

## Research papers

## The influence of hydroclimatic conditions and water quality on evaporation rates of a tropical lake

Janine Brandão de Farias Mesquita<sup>a</sup>, Iran Eduardo Lima Neto<sup>a,\*</sup>, Armin Raabe<sup>b</sup>, José Carlos de Araújo<sup>c</sup><sup>a</sup> Department of Hydraulic and Environmental Engineering, Federal University of Ceará – UFC, Fortaleza, Brazil<sup>b</sup> Leipzig Institute for Meteorology, University of Leipzig, Leipzig, Germany<sup>c</sup> Department of Agricultural Engineering, Federal University of Ceará – UFC, Fortaleza, Brazil

## ARTICLE INFO

This manuscript was handled by Corrado Corradini, Editor-in-Chief

## Keywords:

Evaporation  
Class A pan  
Hydrodynamic modelling  
CE-QUAL-W2  
Water quality  
Correction coefficient

## ABSTRACT

The present paper analyses the influence of hydroclimatic forcing and water quality on the evaporation process of Lake Santo Anastácio, a tropical lake with capacity of about 0.4 hm<sup>3</sup> and maximum depth of 5 m, located in the city of Fortaleza, Ceará, Brazil. The two-dimensional model CE-QUAL-W2 was used for modelling hydrodynamics and direct evaporation from the lake, and an evaporation estimation equation based on the mass transfer method was calibrated. Subsequently, direct evaporation was modelled while, at the same time, thermal characteristics of the water column were examined. Then, modelled evaporation was compared to measurements obtained over a period of 11 years (2009–2019) with a Class A pan. The results indicated a daily thermal stratification of up to 2 °C. When modelled evaporation was compared with the measurements obtained with the Class A pan, the mean Class A pan coefficients (K) were between 0.66 and 0.69, lower than the values reported in literature, possibly due to the high concentration of pollutants in the lake. Finally, the K coefficients were negatively correlated with wind speed (R<sup>2</sup> of 0.51; *p*-value < 0.05), air temperature (R<sup>2</sup> of 0.67; *p*-value < 0.05) and total phosphorus concentration in the dry period (R<sup>2</sup> of 0.41; *p*-value < 0.05); suggesting that wind-induced phosphorus resuspension attenuated evaporation rates in the lake. These results confirm the direct influence of hydroclimatic conditions and water quality on the evaporation rates of a tropical lake. The impact of different K-values on water availability was also investigated. The results of this study are important to assist in management operations of lakes and reservoirs, mainly in regions which are substantially impacted by evaporation, as is the case of the Brazilian semiarid.

## 1. Introduction

The global climatic energy balance depends on the thermal equilibrium between successive changes in the physical state of water, which characterise the many processes involved in the hydrological cycle. One of such processes is evaporation, which begins with the absorption of sensitive heat energy, allowing water temperature to vary until obtaining the amount of energy required to initiate the change of physical state. The completion of the latter requires that additional heat is absorbed, which is known as the latent heat (Abtew and Melesse, 2013; Zhang and Liu, 2014).

In the context of water resource management, the knowledge of evaporation rates is essential to assess the water balance of lakes and surface reservoirs (Biglarbeigi et al., 2018). Yet one of the main challenges when estimating evaporation is the application of precise and

easy-to-use methods, which take into account the numerous variables that influence the environmental systems to be analysed (Majidi et al., 2015; Anda et al., 2016). The need for these methods becomes urgent in water-scarce regions, such as arid and semiarid zones (Ali, Ghosh and Singh, 2008; Majidi et al., 2015; de Araújo et al., 2018), and notably in areas where dense networks of superficial reservoirs have been developed for multiple water uses, as is the case in the state of Ceará, Brazil (Lima Neto et al., 2011; Mamede et al., 2012; de Araújo and Medeiros, 2013; Peter et al., 2014).

In such tropical semiarid regions, water scarcity not only occurs in quantitative but also in qualitative terms, and this makes the evaluation of water availability even more challenging for the respective water bodies (Pacheco and Lima Neto, 2017; Araújo and Lima Neto, 2018; Araújo et al., 2019; Moura et al., 2019). The understanding of the evaporation process is intrinsically linked to quantitative and

\* Corresponding author at: Department of Hydraulic and Environmental Engineering, Federal University of Ceará – UFC, Campus do Pici, bl. 713, Brazil.  
E-mail address: [iran@deha.ufc.br](mailto:iran@deha.ufc.br) (I.E. Lima Neto).

qualitative factors in regions where surface water reserves vary extremely (Lira et al., 2020). This is because evaporation not only reduces the amount of water, but also affects the concentration of substances present in the water bodies (Riveros-Iregui et al., 1997; Havens and Ji, 2018). On the other hand, a higher concentration of substances in a liquid mass also tends to increase the boiling point, decrease vapor pressure and, therefore, reduce evaporation (Andrews, 1976; Calder and Neal, 1984; Hammel, 1994; Oroud, 1995; Ahmadzadeh Kokya et al., 2011; Watras et al., 2016).

Hence, it is necessary to conduct studies that help understand the mechanisms involved in the water evaporation process in natural and artificial water bodies (Zhang and Liu, 2014; Anda et al., 2016; Riveros-Iregui et al., 1997). Moreover, integrated analyses including hydrodynamic and water quality processes should be carried out (Read and Rose, 2013) to develop technically feasible and quantitatively precise tools for the operational management of water resources (Giannou and Antonopoulos, 2007; Majidi et al., 2015).

There are several classic methods and models for the purpose of estimating evaporation, such as: the Class A evaporation pan, the mass transfer methods, Penman, Priestley-Taylor and Bowen's energy-ratio balance (Harbeck, 1962; Bruin, 1974; Warnaka and Pochop, 1988; Singh and Xu, 1997; Ali et al., 2008; McJannet et al., 2012; McGloin et al., 2014; Althoff et al., 2019). Alternatively, previous studies applied one-dimensional hydrodynamic models aimed at interpreting the energy balance and thermal stratification in lakes to estimate evaporation (Hostetler, 1990; Giannou and Antonopoulos, 2007; Helfer et al., 2011; McGloin et al., 2014; Helfer et al., 2018). Some of them compared different methods in order to obtain more accurate correction coefficients for evaporation pans like the Class A pan (Kohler et al., 1955; Neuwirth, 1973; Linacre, 1994; Pereira et al., 2009; Majidi et al., 2015; McJannet et al., 2017; Althoff et al., 2019). Others analysed the thermal effects of varying concentrations of Dissolved Organic Carbon (DOC) in lakes (Read and Rose, 2013), including their impact on evaporation (Watras et al., 2016).

Thus, the present work aims to investigate the influence of hydroclimatic forcing (hydrodynamic and meteorological) and water quality on the evaporation process of a shallow tropical lake located in the northeast of Brazil. It is meant to advance the current state of the art by integrating the following innovative aspects: (1) the application of a two-dimensional hydrodynamic model (CE-QUAL-W2) to analyse evaporation; (2) the evaluation of the influence of hydroclimatic conditions and water quality on lake evaporation rates; and (3) the calculation of linear relationships to describe the evaporation correction coefficients in terms of the variables involved in the phenomenon, using measurements from a Class A pan.

## 2. Methodology

### 2.1. Study area

The study area and object of the present work is Lake Santo Anastácio (coordinates of lake outlet: latitude  $-3.74^{\circ}$  S, longitude  $-38.57^{\circ}$  W), located within the city limits of Fortaleza, state of Ceará, Brazil. It is a coastal region, with an average annual rainfall of 1338 mm concentrated predominantly in the period between January and May, with two defined seasons (rainy and dry) and a sub-humid hot tropical climate, with average temperature ranging from 26 to 28 °C (CEARÁ, 2016), the maximum monthly temperature being 30.7 °C and the minimum monthly temperature, 22.4 °C, an average annual total evaporation of 1435.2 mm and average wind speed of 3.2 m s<sup>-1</sup> (INMET, 2009). Fig. 1 shows the location of Lake Santo Anastácio. The only tributary of the lake is an urban drainage channel with a rectangular section that is 5 m wide and 2.5 km long. It must be mentioned in this context that there are several irregular sewage connections along the channel, added to the base flow from an upstream lake, which keep the water level approximately constant (about 0.2 m) during the dry

season. In Fortaleza, some areas boast a Human Development Index (HDI) of 0.85, while the area around the aforementioned channel has an HDI of approximately 0.35 and can be described as an area of high social vulnerability. Lake Santo Anastácio has a water surface area of 16.00 ± 2.60 ha and depth of 4.79 ± 0.56 m, which makes it a shallow reservoir. Because of eutrophication, the lake water surface is partially (24 ± 6.2%) covered by macrophytes. The above information was extracted from 27 Landsat (5 and 8) satellite images and 35 high-resolution images from Google Earth Pro, including the rainy and dry periods from 2009 to 2020, together with the elevation-area curve of the lake (Fraga et al., 2020). The water is discharged from the lake through a 2.0 m wide Creager spillway. Note that the lake inflow and volume remain approximately constant throughout the days, except for the events of relevant precipitation, because the catchment area is considerably impermeable. As a consequence, during the dry periods, the lake behaves as a nearly steady-state reservoir (Fraga et al., 2020), with coefficients of variation (CV) for the lake surface area and water depth of 8 and 1%, respectively.

### 2.2. Field studies

The hydrological data used in this study was obtained from a meteorological station located approximately 1.0 km from the Lake Santo Anastácio outlet. The station and the lake are located in the Pici Campus of the Federal University of Ceará (UFC). The surroundings of the station and the lake have similar characteristics (buildings of small heights and equivalent vegetation densities). Therefore, we expect no significant differences between the meteorological parameters at the station and the lake. Precipitation, air temperature, wind speed and direction (measured at 10 m above the ground), as well as cloud cover data were obtained three times a day (9.00 am, 3.00 pm and 9.00 pm), between 2009 and 2019. The evaporation data were measured using a standard Class A pan located next to the weather station. It must be highlighted that, over the course of one month, the data generated by that station were compared to two automatic stations installed next to it, so as to guarantee that the station was properly calibrated. Additionally, field campaigns were carried out to measure flow at the inlet and outlet of the lake during 14 days in 2013, as well as for five days in 2018. The equipment used was an electromagnetic propeller flow meter MiniWater20, from Omni Instruments (speed range of 0.02–5.00 m s<sup>-1</sup>), and a ruler, for measurements of water velocity and depth, respectively. This allowed for the calculation of the flow rate.

Water samples were collected from the lake outlet with a Van Dorn bottle, in 2013 (June to December), 2018 (May to December) and 2019 (January to May), totaling 35 samples. The analysed water quality variable was Total Phosphorus (TP). These analyses were carried out at the Chemical Analysis Laboratory (LAQUIM) of the Federal University of Ceará (UFC), using the ascorbic acid method according to Standard Methods (APHA, 2005). Concomitantly with the water sample collection, the temperatures of the lake inflow and outflow were measured by means of a multiparametric probe (HI9820 Hanna Instruments).

### 2.3. Hydrodynamic model

The software used was CE-QUAL-W2 version 3.7, a two-dimensional (2D) hydrodynamic model which considers longitudinal and vertical variations while ignoring lateral variations of hydrodynamic variables (Cole and Wells, 2018). It is suitable for water bodies with great lengths in relation to width and widely applied to study lakes and reservoirs (e.g., Zouabi-Aloui and Gueddari, 2014; Zhang et al., 2018; Ziaie et al., 2019). The model requires data on bathymetry, inflows and outflows, meteorology and water quality (Cole and Wells, 2018). The lake under study was discretised into 32 longitudinal segments of 29 m each and into vertical layers with a layer thickness of 0.2 m, according to the variation of bathymetry.

The analysis period of this work covered eleven years (2009–2019).

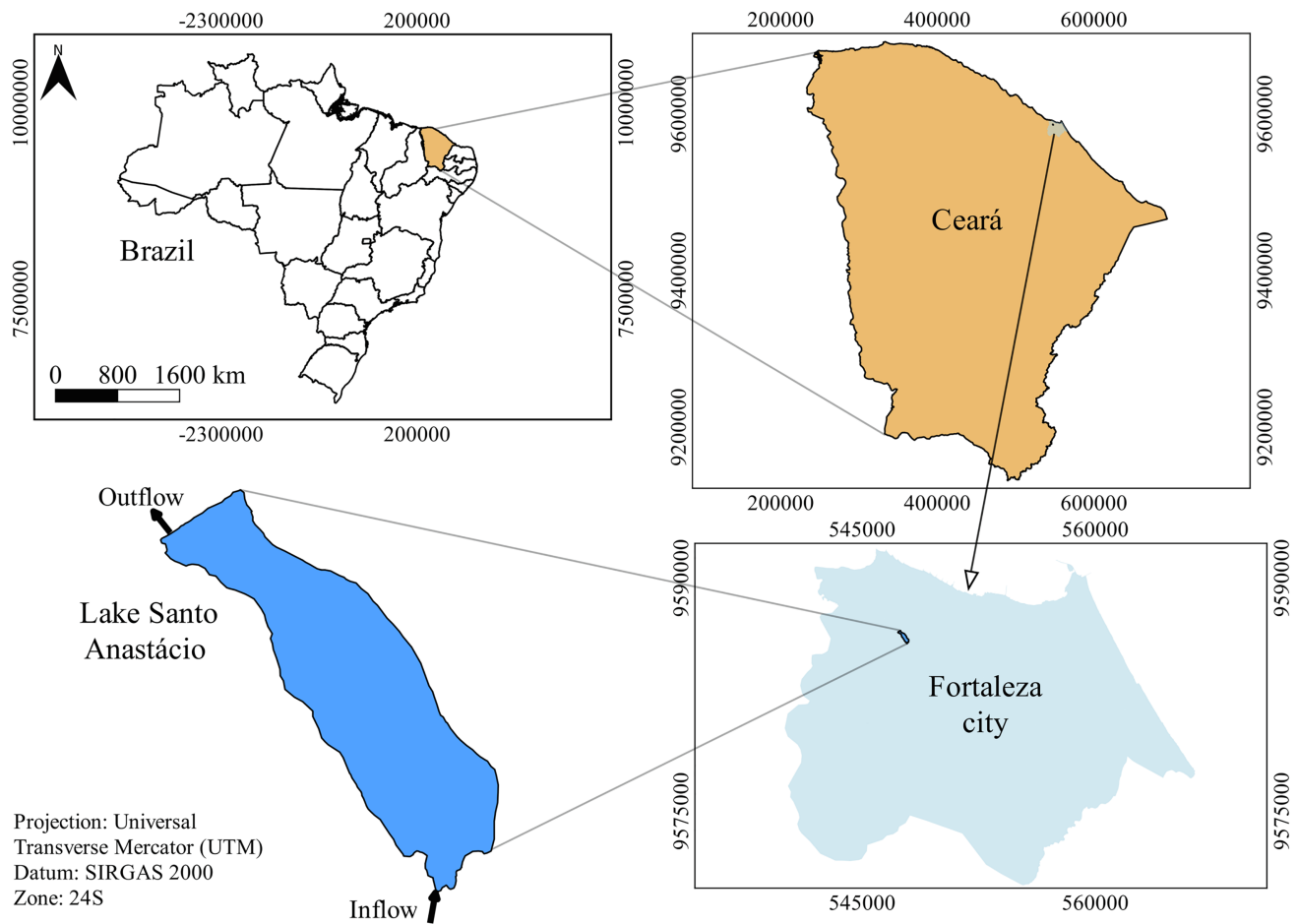


Fig. 1. Location of Lake Santo Anastácio in Fortaleza, Ceará – Brazil. Shapefile source: adapted from Mesquita et al. (2020).

The data input into the model for the corresponding period were meteorological data [air temperature (°C), dew point temperature (°C), wind speed ( $\text{m}\cdot\text{s}^{-1}$ ), wind direction (degrees) and cloud cover (scale from 0 to 10)] measured by the meteorological station; temperature of the inflow and outflow (°C) measured in the field; and flow rates of the lake inlet and outlet ( $\text{m}^3\cdot\text{s}^{-1}$ ), measured monthly in 2013 and 2018 and linearly extrapolated for the remaining days. These features were used to generate the daily flow series required by CE-QUAL-W2, not only for the year 2013, but for all analysed years (2009–2019). It was taken into account that the measurements were made in an intermediate year of the analysed time series (2013). No significant changes in the use and occupation of the contributing basin occurred that could substantially alter the linear relationships adopted (before and after 2013). Additionally, geographic coordinates, bottom elevation (20 m a.s.l.), initial water temperature (28 °C) and sediment temperature (29 °C) were also included in the CE-QUAL W2 model.

Regarding hydraulic parameters, viscosity and wind roughness, standard values for the CE-QUAL-W2 version 3.7 were used (Cole and Wells, 2018). Friction was calculated according to the Chézy equation. It is noteworthy that CE-QUAL-W2 uses the equations of continuity, momentum and heat exchange, and considers the fluid dynamics equations, derived from three-dimensional equations and consisting of six equations and six unknowns, as being laterally constant. Fluid is, thus, considered incompressible, the centripetal acceleration is seen as a small correction of gravity, and the Boussinesq approximation and all velocities and pressures are the sum of turbulent time averages and deviations from the mean (Cole and Wells, 2018).

#### 2.4. Hydrodynamics and evaporation estimation

Among the flow rates measured in 2013 and 2018, those gauged on days without rain were selected. Such consideration can be made given the short concentration time of the basin (less than three hours) (Campos et al., 2020) and its high imperviousness to water, as it is located in a densely urbanised area, so that effects of rainy events from one day do not spread to the following days. According to this rationale, it was possible to estimate the direct evaporation of the lake through the difference between inlet and outlet flow, herein referred to as “calculated evaporation”. The starting point was the premise that there are no inflows or outflows along the lake other than evaporation, and that the lake maintains its level practically constant throughout the year, as observed by Araújo et al. (2019) and Fraga et al. (2020). It was then assumed that there is a balance between groundwater input (G) and infiltration (I), so the difference between G and I would be negligible. What is more, there is no consumptive use of the lake, whose only use is subsistence fishing. Thus, taking the evaporation data calculated in 2013 as reference values, it was possible to calibrate the parameters of a wind function by using the mass transfer method (Dalton's Law) (see Singh and Xu, 1997; Gianniou and Antonopoulos, 2007; López et al., 2012; Alazarda et al., 2015). This method is represented in Eqs. (1) and (2), which are employed by CE-QUAL-W2 to calculate the evaporative heat loss in the lake,  $H_e$  ( $\text{W}\cdot\text{m}^{-2}$ ):

$$H_e = f(u)(e_s - e_a); \text{ and} \tag{1}$$

$$f(u) = a + bu^c; \tag{2}$$

where:  $f(u)$  = wind function ( $\text{W}\cdot\text{m}^{-2}\cdot\text{mmHg}^{-1}$ );  $e_s$  = saturation vapor pressure at the lake surface (mmHg);  $e_a$  = atmospheric vapor pressure

(mmHg);  $a$  ( $\text{W}\cdot\text{m}^{-2}\cdot\text{mmHg}^{-1}$ ),  $b$  ( $\text{W}\cdot\text{m}^{-2}\cdot\text{mmHg}^{-1}\cdot(\text{m}\cdot\text{s}^{-1})^{-c}$ ),  $c$  (dimensionless) = empirical coefficients;  $u$  = wind speed measured at 2 m from the ground outside the lake ( $\text{m}\cdot\text{s}^{-1}$ ). The CE-QUAL-W2 model converts the wind speed from 10 to 2 m using the equations described by Cole and Wells (2018). Moreover, the standard values of the empirical coefficients of the wind function used by CE-QUAL-W2 are from the equation of Edinger et al. (1974), where  $a$ ,  $b$  and  $c$  are  $9.2 \text{ W}\cdot\text{m}^{-2}\cdot\text{mmHg}^{-1}$ ,  $0.46 \text{ W}\cdot\text{m}^{-2}\cdot\text{mmHg}^{-1}\cdot(\text{m}\cdot\text{s}^{-1})^{-c}$  and 2, respectively (Cole and Wells, 2018).

The calibration and validation of the model parameters were performed by statistical analysis, comparing the calculated and modelled evaporation data through mean deviation and determination coefficient ( $R^2$ ). Note that evaporation calculated with data from 2018 was used to validate the model. The thermodynamic method used to calculate heat exchanges consisted of solving Eq. (3) in each discretisation cell of the 2D domain. It is important to highlight that the heat exchanges along the vertical profile depend on water surface temperature. The equations used to calculate each term in Eq. (3) are based on meteorological data and geographic coordinate information, as detailed by Cole and Wells (2018):

$$H_n = H_s + H_a + H_e + H_c - (H_{sr} + H_{ar} + H_{br}); \quad (3)$$

where:  $H_n$  = net heat exchange rate on the water surface ( $\text{W}\cdot\text{m}^{-2}$ );  $H_s$  = incident shortwave radiation ( $\text{W}\cdot\text{m}^{-2}$ );  $H_a$  = incident longwave radiation ( $\text{W}\cdot\text{m}^{-2}$ );  $H_e$  = heat lost in evaporation ( $\text{W}\cdot\text{m}^{-2}$ );  $H_c$  = surface heat conduction ( $\text{W}\cdot\text{m}^{-2}$ );  $H_{sr}$  = reflected shortwave radiation ( $\text{W}\cdot\text{m}^{-2}$ );  $H_{ar}$  = reflected longwave radiation ( $\text{W}\cdot\text{m}^{-2}$ ); and  $H_{br}$  = back radiation from the water surface ( $\text{W}\cdot\text{m}^{-2}$ ). Note that CE-QUAL-W2 calculates incident shortwave radiation ( $H_s$ ) from the relationship between the angle of the sun and cloud cover from the equations described by EPA (1971), Spencer (1971), Wunderlich (1972), Ryan and Stolzenbach (1972), and DiLaura (1984). Moreover, the model considers an exponential decay of shortwave radiation in the water column, according to Bears' Law (Wunderlich, 1972). It should be noted that all terms of the energy balance equation are calculated by CE-QUAL-W2 based on short wave radiation data (Cole and Wells, 2018). The incident longwave radiation from the atmosphere ( $H_a$ ) is obtained by using the Brunt's formula from data of air temperature, cloud cover and air vapor pressure (Brunt, 1932). Heat lost in evaporation ( $H_e$ ) is calculated by Eqs. (1) and (2). Surface heat conduction ( $H_c$ ) is obtained by the product of Bowen's coefficient ( $0.47 \text{ mmHg}\cdot\text{C}^{-1}$ ), the wind function and the air temperature (EPA, 1971). Reflected shortwave radiation ( $H_{sr}$ ), reflected longwave radiation ( $H_{ar}$ ) and back radiation from the water surface ( $H_{br}$ ) are computed using water surface temperature data, water emissivity (0.97) and the Stephan-Boltzman constant ( $5.67 \times 10^{-8} \text{ Wm}^{-2} \text{ K}^{-4}$ ) (EPA, 1971; Wunderlich, 1972). It is noteworthy that the absence of radiometric data directly measured in the lake, and the estimation of the terms of the energy balance equation using only meteorological and geographic coordinate data, is a limitation of the present study. On the other hand, the estimates of the data necessary for the thermal balance, carried out through the equations incorporated in the model, as explained, were sufficient for the complete energy balance. Observe that several previous studies applied the same methodology adopted in the present paper for the energy balance by using the CE-QUAL-W2 model (Deus et al., 2013; Zouabi-Aloui and Gueddari, 2014; Firoozi et al., 2020).

After calibrating and validating the CE-QUAL-W2 model, it was possible to perform hydrodynamic and evaporation simulations for the years 2009 to 2019. To that end, the thermal regime in the water column was interpreted. Therefore, simulations were carried out using the adjusted Eqs. (1) and (2), solving the Eq. (3). Water temperature measurements of Pacheco and Lima Neto (2017) and Lima Neto (2019) were also presented to show the validity of the CE-QUAL-W2 simulations of vertical temperature profiles.

## 2.5. Correction coefficients and hydroclimatic variables

Using simulations of eleven years (2009–2019), time series of daily evaporation were generated for the stratified lake, and they were compared with the measurements in the Class A pan. This way, annual, monthly and seasonal correction coefficients were calculated for the Class A pan (K), as these are commonly used to estimate actual evaporation in water bodies and to obtain greater accuracy in evaporation measurements (e.g., Kohler et al., 1955; Neuwirth, 1973; Linacre, 1994; Pereira et al., 2009; Majidi et al., 2015; Alazarda et al., 2015; Anda et al., 2016; McJannet et al., 2017; Althoff et al., 2019). The annual Class A pan coefficient was obtained by means of linear regression between the respective series of accumulated data for every year (modelled and measured with a Class A pan): this was the slope of the line. Monthly values were obtained in two ways: a generic monthly Class A pan coefficient, obtained by linear regression between measured and modelled evaporation for every month, similar to the annual; and by the relationship between the modelled and measured monthly evaporation. The seasonal Class A pan coefficient was estimated for both the rainy (January to June) and dry (July to December) periods, respectively, by the relationship between modelled and measured evaporation in the corresponding period. After these procedures, correlations were estimated between correction coefficients (K) and meteorological variables in order to analyse the influence of hydroclimatic variables on the measurements of evaporation obtained through a Class A pan.

## 2.6. Correction coefficients and water quality

To analyse the impact of water quality on evaporation, the monthly correction coefficients, obtained through the previously described relationship between modelled and measured evaporation with the Class A pan, were correlated with the monthly average of the total phosphorus variable (or predictor) (TP). The choice of this variable as predictor is justified by the fact that phosphorus is considered the determinant nutrient of the trophic state of the lake under study (see Pacheco and Lima Neto, 2017; Araújo et al., 2019).

As previously mentioned, it is noteworthy that rainfall in the studied region is concentrated between January and May, while the other months of the year are predominantly dry (INMET, 2009). This is why the months of the dry (2013 and 2018) and rainy (2019) periods were segregated for the correlations, in order to minimise possible interferences of meteorological variables in the analysis. Furthermore, it was decided to use the Class A pan coefficient correlated to total phosphorus, since it already incorporates the complexity of meteorological variables in the two systems (lake and Class A pan). Additionally, the meteorological variables were correlated with TP concentration, aiming to understand the factors affecting the physical phenomenon under analysis.

Moreover, an analysis of the impact of evaporation on water availability was carried out using the Vuelas water balance model, which was developed by de Araújo et al. (2006). The hydrological data used for the simulation were those of the 20-year period between 2000 and 2019. Evaporation was estimated using different values of Class A pan coefficients, obtained by interpolating the maximum values of total phosphorus concentration, wind speed and air temperature in the correlation lines mentioned above. A Class A pan coefficient of 0.8 was used as reference value for comparative purposes, as it is commonly used for studies in this region (e.g., Oliveira et al., 2005; Pereira et al., 2009; Campos et al., 2016).

## 3. Results and discussion

### 3.1. Meteorological variables

Fig. 2 shows the distribution of evaporation, precipitation, air



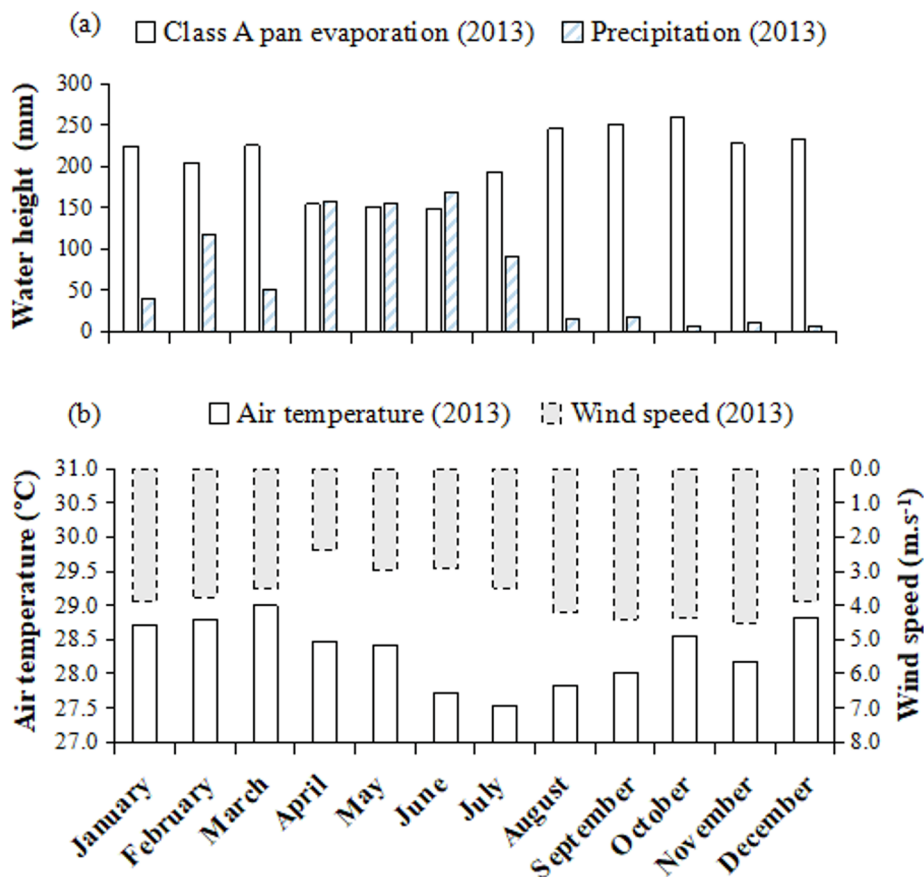


Fig. 2. Monthly distribution (2013) of (a) evaporation and precipitation; and (b) average air temperature and wind speed. Data source: meteorological station from UFC, Ceará, Brazil.

temperature and wind speed throughout 2013 to illustrate the general pattern observed in the region under study. As can be noted, there is a clear seasonality, with evaporation and average wind speed showing predominantly higher values in the second half of the year (July–December), in contrast to higher values for precipitation and average air temperature in the first half (January–May) and reduced rainfall and air temperatures during most months of the second half. De Araújo and Medeiros (2013) describe the hydrological characteristics of the semi-arid region of Northeast Brazil, similarly to the patterns stated in this work. They show that rain is concentrated from January to May, with an average between 500 and 1000 mm·year<sup>-1</sup>; these months are responsible for more than 80% of the annual precipitation, they present average temperatures above 20 °C (usually between 24 and 27 °C) and a potential evaporation of 2500 mm·year<sup>-1</sup>, measured with a Class A pan.

### 3.2. Rainfall and flow data correlations

Fig. 3 exhibits the correlations between rainfall and inflow to and outflow from Lake Santo Anastácio in 2013; these data are used to extrapolate the flows intra and inter annually. It can be seen that linear correlations show a relatively high coefficient of determination ( $R^2 = 0.93$ ;  $p$ -value < 0.05), and this demonstrates the representativeness of the models. Note that Cole and Wells (2018) suggest the use of linear interpolation to fill time series. The proposed correlation considers an increase in flows, however, due to precipitation; this is why it was adjusted to the specific characteristics of the study area.

### 3.3. Model calibration and validation

Table 1 presents the result of the tests of different value

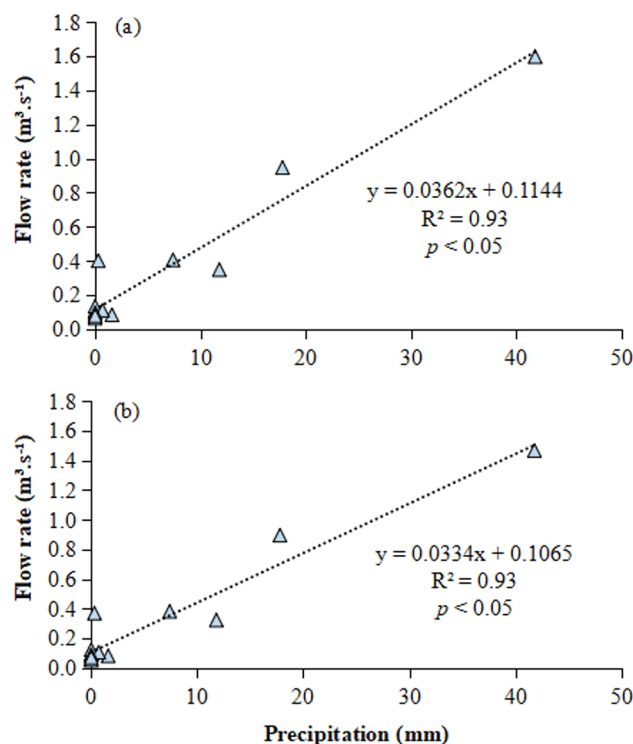


Fig. 3. Correlations between daily precipitation and average daily flow rates at the (a) inlet and (b) outlet of Lake Santo Anastácio in 2013.

**Table 1**

Tested combinations of coefficient values,  $a$  ( $\text{W}\cdot\text{m}^{-2}\cdot\text{mmHg}^{-1}$ ),  $b$  ( $\text{W}\cdot\text{m}^{-2}\cdot\text{mmHg}^{-1}\cdot(\text{m}\cdot\text{s}^{-1})^{-c}$ ) and  $c$  (dimensionless), for the calibration of the wind function, necessary to estimate evaporation in the studied lake.

$c$	$a$	$b$	Mean deviation	Determination coefficient ( $R^2$ ) (calculated and modelled)	$p$ -value	
0.00	18.00	0.00	0.33	0.70	0.8	
	28.00	0.00	0.38	0.63	0.11	
0.5	0.00	2.50	0.66	0.00	0.07	
	3.00	3.50	0.40	0.02	0.13	
	5.00	15.00	0.29	0.84	0.03	
	5.00	18.00	0.29	0.85	0.02	
	5.00	20.00	0.30	0.85	0.03	
	10.00	15.00	0.31	0.77	0.05	
	10.00	20.00	0.33	0.73	0.07	
1.00	0.00	10.00	0.41	0.04	0.72	
	4.00	24.00	0.25	0.18	0.48	
	5.00	20.00	0.26	0.43	0.23	
	6.00	5.00	0.35	0.04	0.09	
	7.00	18.00	0.27	0.78	0.05	
	8.00	17.00	0.28	0.85	0.02	
	<b>8.00*</b>	<b>16.00*</b>	<b>0.28*</b>	<b>0.85*</b>	<b>0.03*</b>	
	8.00	15.00	0.28	0.83	0.03	
	10.00	5.00	0.32	0.11	0.05	
	20.00	2.00	0.28	0.03	0.74	
	20.00	10.00	0.34	0.70	0.08	
	2.00	5.00	15.00	0.32	0.04	0.74
		8.00	16.00	0.29	0.29	0.35
9.20		3.00	0.34	0.72	0.07	
<b>9.20**</b>		<b>0.46**</b>	<b>0.36**</b>	<b>0.71**</b>	<b>0.07**</b>	
16.00		0.46	0.32	0.72	0.07	

\* Coefficients that resulted in the best fit;

\*\* Standard equation coefficients of the model (see Cole and Wells, 2018).

combinations of the coefficients  $a$ ,  $b$  and  $c$  of the adjusted wind function for the evaporation estimation in Lake Santo Anastácio for the dry period of 2013. The analysed statistical parameters (percentage deviation and coefficient of determination) between calculated and modelled evaporation showed that the best fit for the 2013 data was for exponent  $c$  equal to 1 and for coefficients  $a$  and  $b$  equal to  $8 \text{ W}\cdot\text{m}^{-2}\cdot\text{mmHg}^{-1}$  and  $16 \text{ W}\cdot\text{m}^{-2}\cdot\text{mmHg}^{-1}\cdot(\text{m}\cdot\text{s}^{-1})^{-1}$ , respectively (see: Eq. (4)). Between modelled and measured values in 2013, this combination generates an average deviation of 28% and  $R^2$  coefficient of 0.85. Table 1 also shows that most of the other values have a lower coefficient of determination than that obtained with the mentioned values, although some do have a slightly lower deviation. The value of  $c = 1$  corroborates the results of Neuwirth (1973), who states that values of  $c \leq 1$  adapt better to wind speed data for the evaporation estimation. The coefficients  $a$  and  $b$  are within the ranges reported by Cole and Wells (2018).

$$f(u) = 8 + 16u \tag{4}$$

The proposed wind function (Eq. (4)) for the evaporation estimate, when validated with calculated evaporation data for 2018, was obtained by using the same methodology for the evaporation estimate in 2013; it presented an average deviation of 18%, a  $R^2$  coefficient of 0.74 ( $p$ -value of 0.1), and confirms the representativeness of the calibrated model.

Please note that the default equation for the model ( $a = 9.2 \text{ W}\cdot\text{m}^{-2}\cdot\text{mmHg}^{-1}$ ,  $b = 0.46 \text{ W}\cdot\text{m}^{-2}\cdot\text{mmHg}^{-1}\cdot(\text{m}\cdot\text{s}^{-1})^{-2}$ , and  $c = 2$ ) showed a deviation of 36% and an  $R^2$  coefficient of 0.71 ( $p$ -value of 0.07) for 2013 data. For the year 2018, however, despite presenting a 19% deviation, the  $R^2$  coefficient was 0.36 ( $p$ -value of 0.40); this suggests that the default equation is less representative for the investigated region than the adjusted equation (Eq. (4)). Similarly, Singh and Xu (1997) evaluated thirteen equations based on the mass transfer theory to estimate evaporation, and adapted seven generalist equations to stations located in Ontario, Canada: the authors observed that these models were representative when applied to different stations in the

same location yet, when applied to stations in different locations, the models did not represent the measured data. These results confirm the need for wind functions to be adjusted to the respective local conditions and validate the proposition of the present study to develop an equation to estimate evaporation.

Fig. 4 shows the result of the simulations of the adjusted equation in CE-QUAL-W2 for 2013 and 2018 (dry periods). As expected, the adjusted equation (Eq. (4)) presents values below those measured by the Class A pan practically throughout the entire year (see Kohler et al., 1955; Linacre, 1994). It should be remembered in this context that studies which apply CE-QUAL-W2, or other two-dimensional hydrodynamic models, are not identified in literature with the specific purpose of estimating evaporation. Among the studies with computational modelling to adjust the wind function, López et al. (2012) can be mentioned as an example: the authors proposed a methodology which applied Computational Fluid Dynamics (CFD) and aimed to obtain the wind function individually for each analysed system, and an evaporation estimation in Class A pans and water bodies.

### 3.4. Thermal regime of the lake

Simulations with CE-QUAL-W2 of the thermal regime of Lake Santo Anastácio showed temperatures on the water surface vary between approximately 27 and 31 °C during all analysed years (2009–2019), as illustrated in Fig. 5. In addition, it was possible to identify daily (diurnal and nocturnal) thermal stratifications of approximately 1–2 °C. These results are consistent with observations of Pacheco and Lima Neto (2017) and Lima Neto (2019), who experimentally identified the same thermal stratification pattern in the lake (Fig. 6). López Moreira et al. (2018) found a considerable diurnal thermal stratification in Ypacaraí Lake, a shallow subtropical lake in Paraguay, described as a result of high turbidity. Previous studies have also simulated similar thermal behaviors in lakes (see Li et al., 2010; Read and Rose, 2013; Soares et al., 2019).

### 3.5. Class A pan coefficient

Table 2 presents a synthesis of the simulation results for the adjusted equation, displays the annual and monthly Class A pan coefficients which were obtained by linear regression, and the seasonal ones derived through the relationship between modelled and measured values. Fig. 7 illustrates the linear correlations between evaporation (measured by the Class A pan and modelled in CE-QUAL-W2) as obtained for the year 2013.

Normally, a value close to 0.70 is adopted for annual estimates with Class A pan, following the example of Kohler et al. (1955), who estimated the annual correction coefficient for a Class A pan with an average value of 0.70 in the United States of America. Neuwirth (1973) compared values obtained in loco in a shallow lake in Austria with a Class A pan and estimated an average pan coefficient of 0.72 for the analysis period between May and October. Again, in the United States, Linacre (1994) derived a value of 0.70 when relating the averages of twenty months between the evaporation estimated with the Penman method and the Class A pan. Ali et al. (2008) calculated annual Class A pan coefficients between 0.65 and 0.73 (average of 0.65), in a study area in the semiarid region of India. In the northeast of Brazil, in which the lake under study is located, works usually adopt Class A pan coefficients predominantly between 0.60 and 0.90 (Oliveira et al., 2005; Pereira et al., 2009; Mamede et al., 2012; Campos et al., 2016).

The present work evidences, however, annual values for the Class A pan between 0.57 and 0.73 (average of 0.67 and median of 0.66): they are represented by the slope of the line with a null linear coefficient, and their values are slightly below what is commonly suggested in literature (Kohler et al., 1955; Brutsaert and Yeh, 1970; Neuwirth, 1973; Linacre, 1994). The (generic) monthly Class A pan coefficients ranged between 0.59 and 0.70, with an average and median of 0.66; the

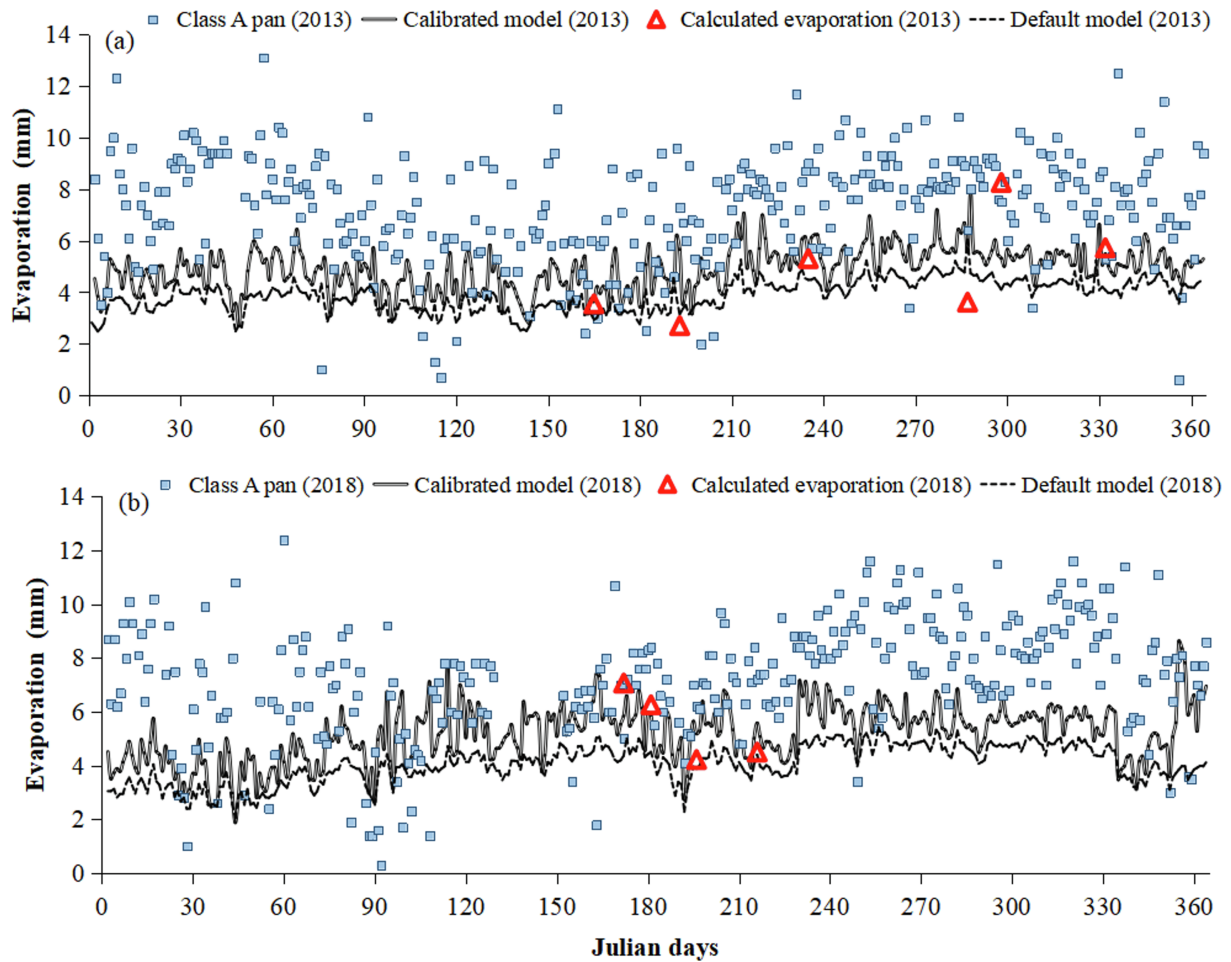


Fig. 4. Modelled evaporation time series (calibrated and CE-QUAL-W2 model default), measured (Class A pan) and calculated by the difference between the inflow to and outflow from the lake in (a) 2013 and (b) 2018.

monthly numbers from relating modelled and measured monthly evaporation varied between 0.49 and 0.84, with averages between 0.56 and 0.72, a general average of 0.67 and a median of 0.68. Althoff et al. (2019) estimated monthly correction coefficients between 0.72 and 0.92 in a small rural reservoir with a surface area of 0.25 ha, located in the Center-West region of Brazil (Brazilian Savannah), by using equations that included meteorological variables and a Class A pan. In a study carried out in an arid region of Australia, McJannet et al. (2017)

estimated a monthly Class A pan coefficient between 0.62 and 0.80 when comparing data from a weather station with simulations using an aerodynamic model. Oliveira et al. (2005) obtained monthly Class A pan coefficients between 0.76 and 0.93 for the semiarid region of Paraíba in Northeastern Brazil.

The seasonal Class A pan coefficients in this work (wet and dry seasons) ranged from 0.61 to 0.75, with an average of 0.69 and 0.66; median of 0.68 and 0.67, respectively. Pereira et al. (2009) estimated

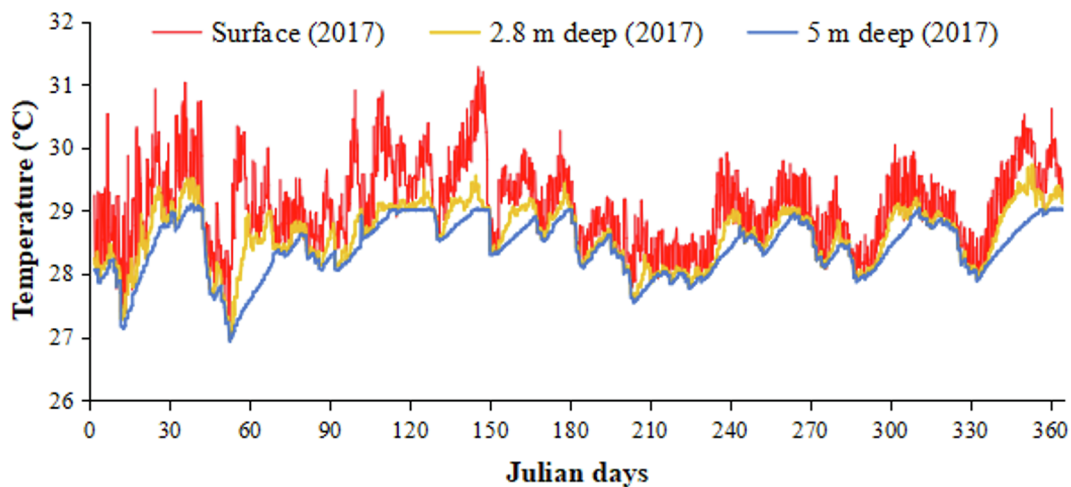


Fig. 5. Daily-water temperature time series of Lake Santo Anastácio at different depths, as simulated by CE-QUAL-W2 for the year 2017.

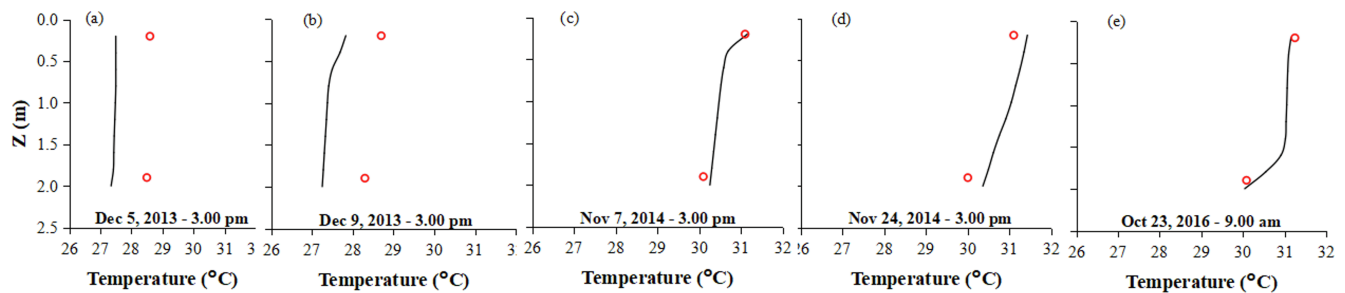


Fig. 6. Comparison of the vertical temperature profile of the water column (Z) modelled by using CE-QUAL-W2 (continuous line) with measured data (circles), from surface to 2 m deep, in Lake Santo Anastácio in (a, b) 2013, (c, d) 2014 and (e) 2016. Measured temperature data: a, b, c, d (Pacheco & Lima Neto, 2017) and e (Lima Neto, 2019).

net evaporation in Sobradinho Lake, located in the São Francisco River Basin (northeast region of Brazil), through measurements with a Class A pan and the models of Linacre (1993), Kohler et al. (1955) and CRLE, and concluded that the seasonal pan coefficient was 0.57. Oliveira et al. (2005), on the other hand, estimated seasonal pan coefficients for the semiarid region of Paraíba, Brazil, and obtained 0.9 and 0.7 for rainy and dry periods, respectively. It is noteworthy in this context that the monthly pan coefficients calculated with the two mentioned methods and the seasonal one, present similar order of magnitude: this suggests that in the study area, seasonality does not affect the Class A pan coefficient as in other regions of Brazilian northeast.

Therefore, the present study showed slightly lower values for Class A pan coefficients than those normally suggested in literature. Morton (1983) also found that pan coefficients of arid regions tend to be lower than those of humid regions. The study area of this work presents high temperatures during practically the whole year (averages of 26 to 28 °C) (INMET, 2009) and a sub-humid hot tropical climate (CEARÁ, 2016). Estimated coefficients are lower, however, than those obtained in arid and semiarid climates, including other parts of Brazil (e.g. Oliveira et al., 2005; McJannet et al., 2017), which suggests the interference of other conditions, in addition to climate.

Fig. 8 shows a comparison between modelled and measured monthly evaporation (Class A pan) in 2013 as an illustration of the general intra-annual pattern. These figures were used to calculate the monthly and seasonal pan coefficients through the relationship between

these variables, as described. There is a clear influence of seasonality on evaporation, because the second semester shows the highest values both in measured and modelled values for all analysed years (2009–2019). Nevertheless, there was no significant impact on the seasonal pan coefficient, as explained. This fact indicates, of course, that there is a proportional reduction and increase between lake evaporation and the measurement with the Class A pan in the rainy and dry period, respectively. Contrastingly, in another study area in the northeast region of Brazil, Oliveira et al. (2005) observed a clear seasonality that impacts the pan coefficient. Linacre (1994) suggested a Class A pan coefficient of 0.77 as a general standard. Still, he warns that several factors can change this value, including evaporation rates, which are a function of latitude, solar declination, cloud cover and aridity of the environment. Therefore, the pattern of proportionality between evaporation in lakes and pans is directly linked to the climate of the study region, among other aspects. This fact justifies the particular trends to be discussed in the following section.

### 3.5.1. Correlation between pan coefficients and meteorological variables

By the correlation between the annual Class A pan coefficients for the eleven year period with annual average air temperature (°C) and annual average wind speed (ms<sup>-1</sup>), as shown in Fig. 9, a negative correlation could be found: R<sup>2</sup> of 0.51 (p-value < 0.05) and 0.67 (p-value < 0.05), respectively. It may be inferred that this correlation exists due to the tendency of the Class A pan to enhance evaporation in

Table 2

Class A pan coefficients (annual, monthly and seasonal) and statistical analysis (data measured and modelled in CE-QUAL-W2) for simulations between 2009 and 2019.

Year	DM <sup>1</sup> (%)	R <sup>2</sup> (calculated vs. modelled) <sup>2</sup>	K <sub>annual</sub> <sup>3</sup>	R <sup>2</sup> (K <sub>annual</sub> ) <sup>*</sup>	p-value	K <sub>monthly generic</sub> <sup>4</sup>	R <sup>2</sup> (K <sub>monthly</sub> ) <sup>*</sup>	p-value	K <sub>monthly</sub> <sup>5</sup> (average)	K <sub>seasonal</sub> <sup>6</sup>	
										Wet	Dry
2009	–	–	0.72	0.99	0	0.70	0.94	1.78.10 <sup>-7</sup>	0.72	0.73	0.70
2010	–	–	0.57	0.99	0	0.59	0.94	7.90.10 <sup>-8</sup>	0.56	0.72	0.61
2011	–	–	0.70	0.99	0	0.68	0.96	1.67.10 <sup>-8</sup>	0.70	0.73	0.67
2012	–	–	0.66	0.99	0	0.65	0.78	6.23.10 <sup>-5</sup>	0.66	0.67	0.65
2013	0.28	0.85	0.67	0.99	0	0.67	0.81	3.64.10 <sup>-5</sup>	0.68	0.66	0.69
2014	–	–	0.63	0.99	0	0.64	0.98	2.00.10 <sup>-9</sup>	0.68	0.63	0.64
2015	–	–	0.64	0.99	0	0.65	0.93	3.97.10 <sup>-7</sup>	0.64	0.61	0.67
2016	–	–	0.66	1.00	0	0.66	0.90	2.17.10 <sup>-6</sup>	0.65	0.65	0.66
2017	–	–	0.65	0.99	0	0.63	0.98	1.43.10 <sup>-10</sup>	0.66	0.68	0.63
2018	0.18	0.74	0.71	0.99	0	0.69	0.79	6.63.10 <sup>-5</sup>	0.71	0.75	0.67
2019	–	–	0.73	0.99	0	0.70	0.96	8.03.10 <sup>-8</sup>	0.71	0.72	0.70
Average	–	–	0.67	0.99	0	0.66	0.91	1.53.10 <sup>-5</sup>	0.67	0.69	0.66
Median	–	–	0.66	–	–	0.66	–	–	0.68	0.68	0.67

<sup>1</sup> DM (mean deviation between modelled and measured values);

<sup>2</sup> R<sup>2</sup> (determination coefficient between modelled and measured values);

<sup>3</sup> K<sub>annual</sub> (annual pan coefficient – straight slope);

<sup>\*</sup> R<sup>2</sup> (corresponding coefficient of determination);

<sup>4</sup> K<sub>generic monthly</sub> (monthly pan coefficient – straight slope);

<sup>5</sup> K<sub>monthly</sub> (monthly pan coefficient obtained from the relationship between modelled and measured values);

<sup>6</sup> K<sub>seasonal</sub> (seasonal pan coefficient calculated from the relationship between modelled and measured data).



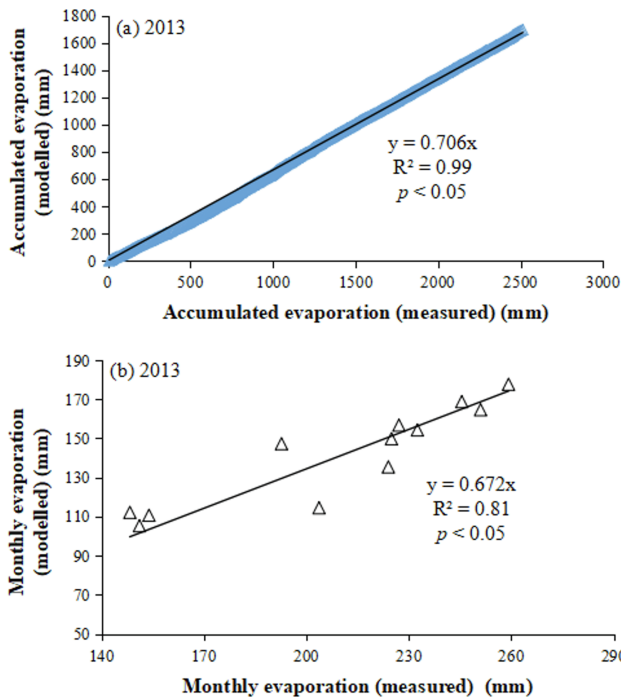


Fig. 7. Linear regression for the year 2013 between the accumulated annual evaporation data measured in a Class A pan and modelled in CE-QUAL W2 (a), and between the monthly evaporation data measured in the Class A pan and modelled in CE-QUAL W2 (b), so as to obtain the annual ( $K_a$ ) and generic monthly ( $K_m$ ) Class A pan coefficient, respectively (straight slope).

dry periods, mainly because of the aforementioned meteorological variables, since the equipment consists of a metallic pan which favors the occurrence of such a phenomenon (Linacre, 1994). In periods of more substantial precipitation, lower wind speeds and air temperature, though, the opposite phenomenon can be observed. Note that the effect of wind speed on phosphorus re-suspension will also be discussed later in this paper (see Section 3.5.2). This particularity indicates that the meteorological factor is directly related to measurement variations of the Class A pan and, therefore, to the annual pan coefficient to be adopted (Morton, 1986). Linacre (1994) draws attention to the fact that Class A pan coefficients are strongly influenced not only by the geometry of the equipment, which interferes with energy irradiation, but also by climate characteristics of the studied region, such as the aridity

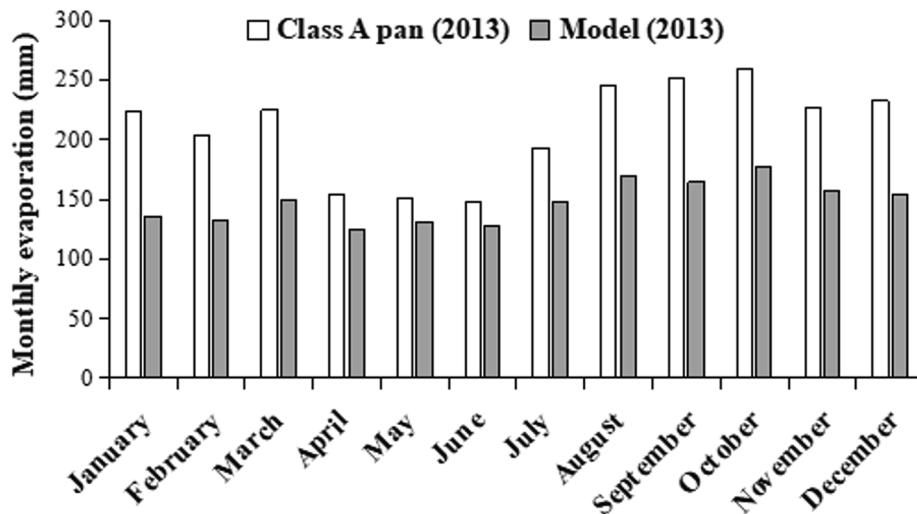


Fig. 8. Comparison between the monthly evaporation data (mm) in 2013 measured in the Class A pan and modelled in CE-QUAL-W2; this data was used to calculate the monthly and seasonal Class A pan coefficients.

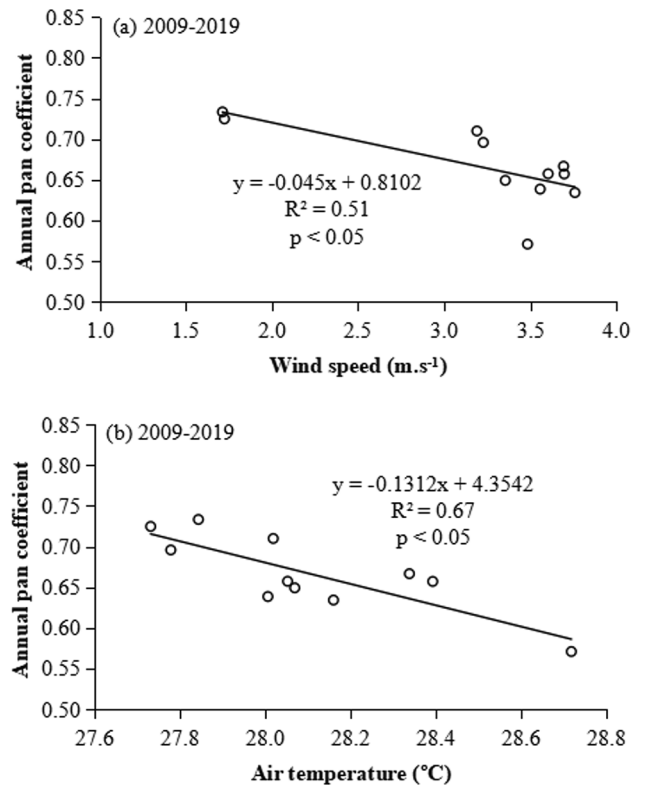


Fig. 9. Linear regression between the annual Class A pan coefficient and (a) the average annual wind speed ( $m\cdot s^{-1}$ ); and (b) average annual temperature ( $^{\circ}C$ ) (straight slope) during the eleven analysed years (2009–2019).

of the environment. Morton (1983) states that traditional evaporation estimation techniques depart from the assumption that evaporation can be estimated in different environments by applying a simple coefficient transposed from one place to another. At the same time the author pointed out that Hounam (1973) obtained several annual Class A pan coefficients in different lakes where annual rainfall was quite variable, such as a  $K_a$  coefficient equal to 0.81 for an average annual precipitation of 1400 mm; 0.7 for 800 mm and 0.52 for approximately 60 mm precipitations. These examples confirm the trends detected in this work with regards to variations of the correction coefficients as being proportional to weather conditions. Moreover, the present study

demonstrates variability of the  $K_a$  coefficient in the same study area, depending on meteorological variables: a finding that highlights the sensitivity of this parameter to local peculiarities (Linacre, 1994).

With regards to seasonality, the following data were obtained: correlations with average annual wind speed ( $\text{m}\cdot\text{s}^{-1}$ ) and average annual air temperature ( $^{\circ}\text{C}$ ) with  $R^2$  coefficients of 0.44 ( $p$ -value  $< 0.05$ ) and 0.08 ( $p$ -value of 0.39), for the rainy season, and of 0.19 ( $p$ -value of 0.18) and 0.36 ( $p$ -value of 0.05), for the dry season, respectively. It can be seen, through the non-significant statistical results, that there is no relevant correlation between the wind speed (dry period), the air temperature (rainy period), and the seasonal Class A pan coefficients. These results express that on a smaller time scale, in this case seasonal, the relationship between variability in the Class A pan coefficient and the climate shows an average correlation only in the rainy season for wind speed and in the dry period for air temperature. Yet the relationship between seasonal Class A pan coefficients and the meteorological variables is not direct and considerable, unlike on a larger scale such as the annual one, as was demonstrated. It is important to highlight that in literature no studies with similar correlations could be found.

### 3.5.2. Correlation between pan coefficient and water quality

Fig. 10 shows the correlation between the monthly average of total phosphorus concentration (TP) and the monthly Class A pan coefficients for the dry (2013 and 2018) and rainy (2019) periods. It appears that the pan coefficient decreases as the concentration of TP increases, since the  $R^2$  coefficient is 0.41 ( $p$ -value  $< 0.05$ ) and 0.27 ( $p$ -value of 0.37) for the dry and rainy periods, respectively. This finding reveals the impact of water quality on reducing evaporation from the lake. Another aspect to be considered is the influence of seasonality on the quality of the lake water, with higher and lower concentrations of total phosphorus during the dry and rainy periods, respectively. This fact is a reminder that these periods need to be segregated for the observation of the phenomenon under analysis. In addition, the correlation between the TP concentration and the Class A pan coefficient is not statistically

significant for the rainy season ( $R^2$  of 0.27;  $p$ -value of 0.37), probably due to the small number of data points, relevant variability of weather conditions, and relatively low values of TP concentration. Note that the high level of TP observed in this study is a clear indicator that there are other substances and microorganisms in the lake water (for example, organic matter and bacteria), as verified by past studies (Araújo and Lima Neto, 2018; Araújo et al., 2019; Fraga et al., 2020). This suggests that the other substances and microorganisms in the lake can also affect the evaporation process, either directly or through secondary processes, such as eutrophication.

The influence of TP concentration on evaporation rates may explain why Class A pan coefficients are lower than those reported in the literature. And may also suggest that this variable can be reduced in the presence of a high pollutant load, as is normally the case in urban lakes and was also verified for the hypereutrophic Lake Santo Anastácio (Pacheco and Lima Neto, 2017; Araújo and Lima Neto, 2018; Araújo et al., 2019). A relevant aspect caused by water pollution is the reduction of light penetration in the liquid mass due to high turbidity that normally characterises hypereutrophic surface water bodies (Havens and Ji, 2018) and increases the albedo (Jin et al., 2004), along with floating macrophytes that can also prevent the passage of light. On the other hand, the presence of certain species of aquatic macrophytes can increase surface water losses through evapotranspiration (Jiménez-Rodríguez et al., 2019). Classically in studies on evaporation, turbidity is pointed out as an analytical parameter that indicates a reduction of evaporation as it rises (Morton, 1986; Finch and Hall, 2001). Still, other limnological variables should also be evaluated as they, too, can influence the energy balance and, consequently, the evaporative process: examples include submerged macrophytes, water colour (related to DOC concentration), the depth of the water column and the characteristics of the sediments (Herb and Stefan, 2004; Persson and Jones, 2008; Rinke et al., 2010). These caveats suggest a potential topic for further research.

Anda et al. (2016), for instance, performed experiments and compared evaporation in two Class A pans: the first, a standard Class A pan; the second, with submerged macrophytes and sediment cover at the bottom. These authors observed that evaporation in the second pan was higher than in the first, probably due to the greater energy absorption of the dark color, an effect of the presence of macrophytes and sediment. Read and Rose (2013), on the other hand, applied a one-dimensional thermodynamic model to eight shallow lakes in Wisconsin and Michigan, in the United States, and analysed the dissolved organic carbon (DOC): they found that an increase in DOC concentration favors a decrease in the overall heat content by blocking the penetration of light into the water column and, consequently, a reduction in the general temperature of the lake. The authors also found an increase in the outward heat fluxes, which would tend to damp evaporation, because this is one of the terms of the energy balance. Oroud (1995) observed an increase in the water temperature, although in his study it was related to an increase in salinity. More recently, Watras et al. (2016) studied the influence of dissolved organic carbon (DOC) on the evaporation of three shallow lakes in Wisconsin, United States. The authors found that although the presence of DOC is related to the elevation of lake surface temperature, it does not imply an increase in evaporation, but its reduction. They suggested two mechanisms to explain this effect: disproportionate emission of radiant energy by lakes with high DOC concentrations, and the combined effect of wind speed and vapor pressure gradient, of which the product is lower in lakes with the described features.

It can, hence, be inferred that high polluting loads in water bodies may alter the process of direct evaporation, and this mechanism should not be analysed only from the perspective of climatic variables (Zhang and Liu, 2014). To measure evaporation data using a Class A pan it is, therefore, necessary to adopt pan coefficients which coherently represent the system, incorporate aspects related to water quality (Boyd, 1985; Oroud, 1995) and, consequently, contribute to a proper

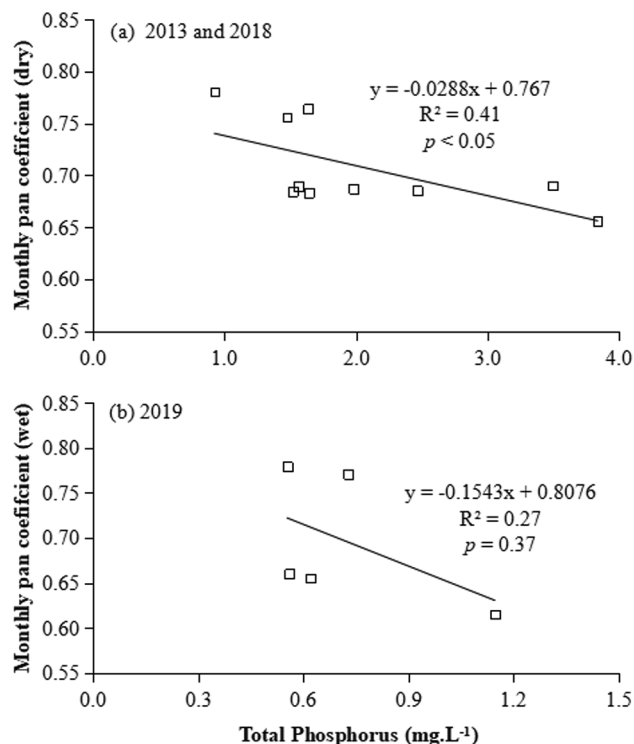


Fig. 10. Linear regression between the monthly average of Total Phosphorus concentration (TP) ( $\text{mg}\cdot\text{L}^{-1}$ ) and monthly Class A pan coefficients for (a) the dry (2013 and 2018) and (b) rainy periods (2019).

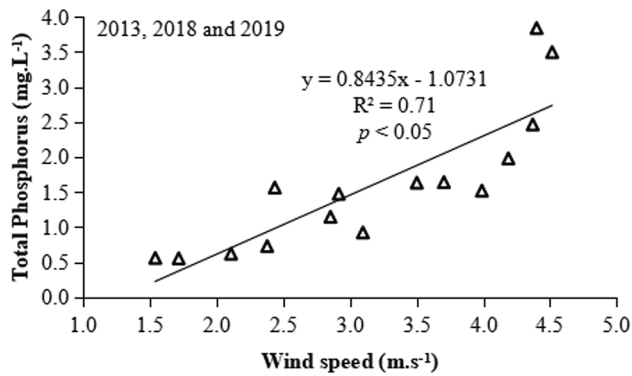


Fig. 11. Linear regression between Total Phosphorus concentration (TP) and wind speed including both the dry (2013 and 2018) and rainy periods (2019).

estimation of the water balance, especially in lentic environments. The need for further studies that consider the complexity of the involved variables must also be emphasised, in order to deepen this area of knowledge.

Fig. 11 shows a linear regression between total phosphorus concentration and wind speed including both the dry (2013 and 2018) and rainy periods (2019). The direct dependence of TP on wind speed ( $R^2$  of 0.71;  $p$ -value < 0.05) confirms that wind-induced sediment/phosphorus resuspension was an important process, as pointed out by Araújo et al. (2019). This suggests that the impact of the wind speed on water quality was the dominant factor damping evaporation rates in the lake, as compared to those at the Class A pan. Observe that this analysis also provided a new empirical correlation to estimate the total phosphorus concentration in the lake.

Finally, Fig. 12 shows a comparison of water availability simulations in Lake Santo Anastácio, which were estimated by using the Vyelas model (de Araújo et al., 2006) for different evaporation values calculated with Class A pan coefficients of 0.80, 0.68, 0.63 and 0.58, that had been obtained in correlations with TP concentration, wind speed and air temperature, respectively. A reduction in evaporation rates of 15, 21 and 28% could be observed; attained with the last three coefficients in relation to the Class A pan coefficients of 0.80. This implied an average increase in water availability of 18.24, 24.25 and 29.50%, respectively, evidencing the high sensitivity of the water reliability estimate to the employed evaporation rates and, consequently, to the pan coefficient for the case of estimations which use evaporation data measured with a Class A pan.

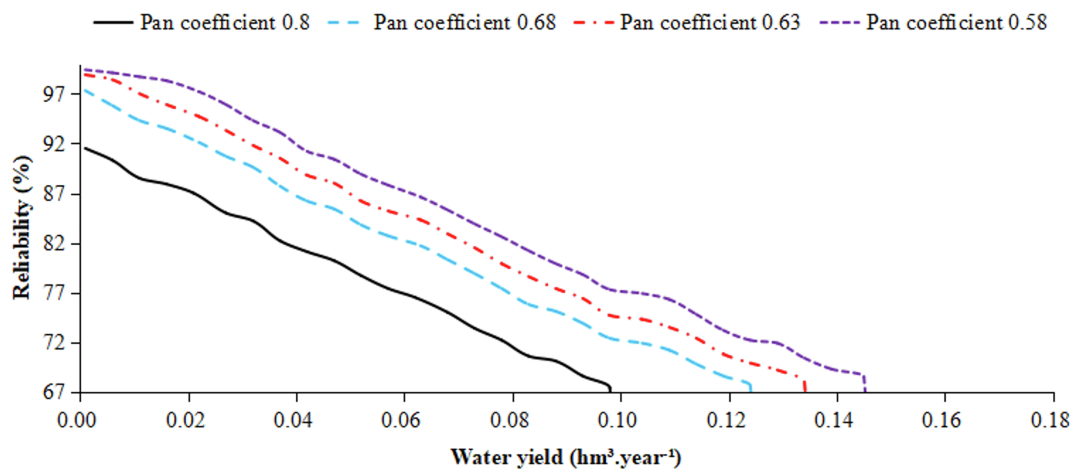


Fig. 12. Simulation of water availability (2000–2019) for different evaporation values estimated with Class A pan coefficients (0.80, 0.68, 0.63 and 0.58 represent the standard value in literature and those obtained by the correlation with Total Phosphorus concentration (TP), wind speed and air temperature, respectively), for Lake Santo Anastácio, in Fortaleza, Ceará, Brazil.

#### 4. Conclusions

The present work analysed the influence of hydroclimatic forcing agents on the evaporation process of a tropical urban lake. Considering the results obtained, it can be concluded that the lake presented mild thermal stratification of the water column, from 1 to 2 °C, despite its shallowness, which demonstrates that the energy distribution in the water column is not uniform. It was also found that annual, monthly and seasonal Class A pan coefficients showed lower values than those obtained in literature. There was, moreover, a strong negative correlation between the annual Class A pan coefficients and meteorological variables (wind speed and air temperature), suggesting that Class A pan-based methods tend to overestimate evaporation measurements, depending on weather conditions.

Additionally, it was observed that a higher concentration of total phosphorus potentially resulted in a lower monthly Class A pan coefficient, a fact that suggests the influence of water quality on evaporation in the studied tropical reservoir. The results also indicated that wind-induced sediment/phosphorus re-suspension potentially attenuated evaporation rates in the lake. Moreover, the impact of evaporation on water availability could be proven: reductions in evaporation above 15% implied an increase in water availability in the same proportion.

Finally, we may say that it is essential to adopt tools which can provide an integrated analysis and to verify meteorological and hydrodynamic processes and water quality, in order to achieve greater accuracy when estimating the evaporation process in lakes and reservoirs, and to guarantee the effective operation and management of such water bodies.

#### CRediT authorship contribution statement

**Janine Brandão de Farias Mesquita:** Data curation, Formal analysis, Methodology, Writing - original draft, Software. **Iran Eduardo Lima Neto:** Conceptualization, Funding acquisition, Methodology, Supervision, Writing - review & editing. **Armin Raabe:** Writing - review & editing. **José Carlos de Araújo:** Conceptualization, Funding acquisition, Methodology, Writing - review & editing.

#### Declaration of Competing Interest

The authors declare that they have no known competing financial interests or personal relationships that could have appeared to influence the work reported in this paper.

## Acknowledgements

The work undertaken for this investigation was supported by the Coordination for the Improvement of Higher Education Personnel – CAPES (Research Grant PROEX 20/2016; and PRINT, Grant 8881.311770/2018-01), and the Ceará State Research Foundation – FUNCAP (Research Grant PNE-0112-00042.01.00/16).

## References

- Abtew, W., Melesse, A., 2013. In: *Evaporation and Evapotranspiration: Estimations and Measurements*. Springer, Dordrecht Heidelberg New York London. <https://doi.org/10.1007/978-94-007-4737-1>. ISBN 978-94-007-4737-1 (eBook).
- Ahmadzadeh Kokya, T., Pejman, A.H., Mahin Abdollahzadeh, E., Ahmadzadeh Kokya, B., Nazariha, M., 2011. Evaluation of salt effects on some thermodynamic properties of Urmia Lake water. *Int. J. Environ. Res.* 5 (2), 343–348.
- Alazarda, M., Leduc, C., Travi, Y., Boulet, G., Ben Saleme, A., 2015. Estimating evaporation in semi-arid areas facing data scarcity: example of the El Haouareb dam (Merguellil catchment, Central Tunisia). *J. Hydrol.: Reg. Stud.* 3, 265–284. <https://doi.org/10.1016/j.ejrh.2014.11.007>.
- Ali, S., Ghosh, N.C., Singh, R., 2008. Evaluating best evaporation estimate model for water surface evaporation in semi-arid region, India. *Hydrol. Process* 22, 1093–1106.
- Althoff, D., Rodrigues, L.N., Silva, D.D., Bazame, H.C., 2019. Improving methods for estimating small reservoir evaporation in the Brazilian Savanna. *Agric. Water Manage.* 216, 105–112. <https://doi.org/10.1016/j.agwat.2019.01.028>.
- Anda, A., Simon, B., Soos, G., Teixeira da Silva, J.A., Kucserka, T., 2016. Effect of submerged, freshwater aquatic macrophytes and littoral sediments on pan evaporation in the Lake Balaton region, Hungary. *J. Hydrol.* 542, 615–626. <https://doi.org/10.1016/j.jhydrol.2016.09.034>.
- Andrews, F.C., 1976. Colligative properties of simple solution. *Science* 194 (4195), 567–571. <https://doi.org/10.1126/science.194.4265.567>.
- APHA. *American Public Health Association, 2005. Standard Methods for the Examination of Water and Wastewater*, 21th. ed. American Public Health Association/American Water Works Association/Water Environment Federation, Washington, USA.
- Araújo, G.M., Lima Neto, I.E., 2018. Removal of organic matter in stormwater ponds: a plug flow model generalisation from waste stabilisation ponds to shallow rivers. *Urban Water J.* 15 (9), 918–924. <https://doi.org/10.1080/1573062X.2019.1581231>.
- Araújo, G.M., Lima Neto, I.E., Becker, H., 2019. Phosphorus dynamics in a highly polluted urban drainage channel shallow reservoir system in the Brazilian semiarid. *Ann. Braz. Acad. Sci.* 91 (3). <https://doi.org/10.1590/0001-3765201920180441>.
- Biglarbeigi, P., Giuliani, M., Castelletti, A., 2018. Partitioning the impacts of streamflow and evaporation uncertainty on the operations of multipurpose reservoirs in arid regions. *J. Water Resour. Plann. Manage.* 144 (7). [https://doi.org/10.1061/\(ASCE\)WR.1943-5452.0000945](https://doi.org/10.1061/(ASCE)WR.1943-5452.0000945).
- Boyd, C.E., 1985. Pond evaporation. *Trans. Am. Fish. Soc.* 114 (2), 299–303. [https://doi.org/10.1577/1548-8659\(1985\)114<299:PE>2.0.CO;2](https://doi.org/10.1577/1548-8659(1985)114<299:PE>2.0.CO;2).
- Bruin, H.A.R., 1974. A simple model for Shallow Lake evaporation. *J. Appl. Meteorol.* 17, 1132–1134. [https://doi.org/10.1175/1520-7010450\(1978\)017<1132:ASMFSL>2.0.CO;2](https://doi.org/10.1175/1520-7010450(1978)017<1132:ASMFSL>2.0.CO;2).
- Brunt, D., 1932. Notes on radiation in the atmosphere I. *Q. J. Resour. Meteorol. Soc.* 58 (247), 389–418. <https://doi.org/10.1002/qj.49705824704>.
- Brutsaert, W., Yeh, G.T., 1970. Implications of a type of empirical evaporation formula for lakes and pans. *Water Resour. Res.* 6 (4), 1202–1208. <https://doi.org/10.1029/wr006i004p01202>.
- Calder, I.R., Neal, C., 1984. Evaporation from saline lakes: a combination equation approach. *Hydrol. Sci. J.* 29 (1), 89–97. <https://doi.org/10.1080/02626668409490924>.
- Campos, J.N.B., Lima Neto, I.E., Studart, T.M.C., Nascimento, L.S.V., 2016. Trade-off between reservoir yield and evaporation losses as a function of lake morphology in semiarid Brazil. *Ann. Braz. Acad. Sci.* 88, 1113–1126.
- Campos, J.N.B., Rabelo, U.P., Lima Neto, I.E., 2020. The bell-shaped unit hydrograph for overlaid planes. *J. Irrig. Drain. Eng.* 146 (5), 1–6. [https://doi.org/10.1061/\(ASCE\)IR.1943-4774.0001465](https://doi.org/10.1061/(ASCE)IR.1943-4774.0001465).
- Ceará. Instituto de Pesquisa e Estratégia Econômica do Ceará, 2016. Perfil Básico Municipal. Fortaleza.
- Cole, T.M., Wells, S.A., 2018. CE-QUAL-W2: A Two-Dimensional, Laterally Averaged, Hydrodynamic and Water Quality Model, Version 4.1. Portland State University, Portland.
- de Araújo, J.C., Güntner, A., Bronstert, A., 2006. Loss of reservoir volume by sediment deposition and its impact on water availability in semiarid Brazil. *Hydrol. Sci. J.* 51 (1), 157–170.
- de Araújo, J.C., Medeiros, P.H.A., 2013. Impact of dense reservoir networks on water resources in semiarid environments. *Aust. J. Water Resour.* 17 (1), 87.
- de Araújo, J.C., Mamede, G.L., Lima, B.P., 2018. Hydrological guidelines for reservoir operation: application to the Brazilian Semiarid region. *Water* 10, 1628. <https://doi.org/10.3390/w10111628>.
- Deus, R., Brito, D., Mateus, M., Kenov, I., Fornaro, A., Neves, R., Alves, C.N., 2013. Impact evaluation of a pisciculture in the Tucuruí reservoir (Pará, Brazil) using a two-dimensional water quality model. *J. Hydrol.* 487, 1–12. <https://doi.org/10.1016/j.jhydrol.2013.01.022>.
- DiLaura, D.L., 1984. Recommended practice for the calculation of daylight availability. *J. Illum. Eng. Soc. N. Am.* 13 (4), 381–392. <https://doi.org/10.1080/00994480.1984.10748791>.
- Edinger, J.E., Brady, D.K., Geyer, J.C., 1974. Heat Exchange and Transport in the Environment, Rpt. No. 14, EPRI Publication No. 74-049-00-34, Electric Power Research Institute, Cooling Water Discharge Research Project RP-49, Palo Alto, CA.
- EPA. Environmental Protection Agency, 1971. Effect of Geographical Location on Cooling Pond Requirements and Performance, in *Water Pollution Control Research Series*. Report No. 16130 FDQ, Environmental Protection Agency, Water Quality Office, Washington, District of Columbia, 160 pp.
- Finch, J.W., Hall, R.L., 2001. Estimation of Open Water Evaporation. *Environ Agency, Bristol*.
- Firoozi, F., Roobahani, A., Bavani Massah, A.R., 2020. Developing a framework for assessment of climate change impact on thermal stratification of dam reservoirs. *Int. J. Environ. Sci. Technol.* 17, 2295–2310. <https://doi.org/10.1007/s13762-019-02544-8>.
- Fraga, R.F., Rocha, S.M.G., Lima Neto, I.E., 2020. Impact of flow conditions on coliform dynamics in an urban lake in the Brazilian semiarid. *Urban Water J.* 17 (1), 43–53. <https://doi.org/10.1080/1573062X.2020.1734948>.
- Giannou, S.K., Antonopoulos, V.Z., 2007. Evaporation and energy budget in Lake Vegoritis, Greece. *J. Hydrol.* 345, 212–223. <https://doi.org/10.1016/j.jhydrol.2007.08.007>.
- Hammel, H.T., 1994. How solutes alter water in aqueous solutions. *J. Phys. Chem.* 98 (15), 4196–4204. <https://doi.org/10.1021/j100066a046>.
- Harbeck, G.E., 1962. A Practical Field Technique for Measuring Reservoir Evaporation Utilizing Mass-transfer Theory. U.S. Geological Survey Prof. Paper 272E.
- Havens, K.E., Ji, G., 2018. Multiyear oscillations in depth affect water quality in Lake Apopka. *Inland Waters.* 8 (1), 1–9. <https://doi.org/10.1080/20442041.2018.1428429>.
- Helfer, F., Zhang, H., Lemckert, C., 2011. Modelling of lake mixing induced by air bubble plumes and the effects on evaporation. *J. Hydrol.* 406, 182–198.
- Helfer, F., Andutta, F.P., Louzada, J.A., Zhang, H., Lemckert, C., 2018. Artificial destratification for reducing reservoir water evaporation: is it effective? *Lakes Reservoirs Res. Manage.* <https://doi.org/10.1111/lre.12241>.
- Herb, W.R., Stefan, H.G., 2004. Temperature stratification and mixing dynamics in a Shallow Lake with submersed macrophytes. *Lake Reservoir Manage.* 20 (4), 296–308. <https://doi.org/10.1080/07438140409354159>.
- Hostetler, S.W., 1990. Simulation of Lake evaporation with application to modeling lake level variations of Harney-Malheur Lake, Oregon. *Water Resour. Res.* 26 (10), 2603–2612. <https://doi.org/10.1002/hyp.6664>.
- Hounan, C.E., 1973. Comparison between pan and lake evaporation. *World Meteorol. Org. (W.M.O.), Geneva, Tech. Note No. 126*, p. 15.
- INMET. Instituto Nacional de Meteorologia. Normais Climatológicas do Brasil 1961-1990. Organizadores: RAMOS, Andrea Malheiros; SANTOS, Luiz André Rodrigues dos; FORTES, Lauro Tadeu Guimarães. Brasília-DF: INMET, 2009.
- Jiménez-Rodríguez, C., Esquivel-Vargas, C., Coenders-Gerrits, M., Sasa-Marín, M., 2019. Quantification of the evaporation rates from six types of wetland cover in Palo Verde National Park, Costa Rica. *Water* 11 (4), 674. <https://doi.org/10.3390/w11040674>.
- Jin, Z., Charlock, T.P., Smith, W.L., Rutledge, K., 2004. A parameterization of ocean surface albedo. *Geophys. Res. Lett.* 31 (22). <https://doi.org/10.1029/2004gl021180>.
- Kohler, M., Nordenson, T., Fox, W., 1955. *Evaporation from Pans and Lakes: US Weather Bureau Research Paper 38*. US Weather Bureau, Washington, DC.
- Li, Y., Acharya, K., Chen, D., Stone, M., 2010. Modeling water ages and thermal structure of Lake Mead under changing water levels. *Lake Reservoir Manage.* 26, 258–272. <https://doi.org/10.1080/07438141.2010.541326>.
- Lima Neto, I.E., 2019. Impact of artificial destratification on water availability of reservoirs in the Brazilian semiarid. *Ann. Braz. Acad. Sci.* 91 (3), 1–12. <https://doi.org/10.1590/0001-3765201920171022>.
- Lima Neto, I.E., Wiegand, M.C., de Araújo, J.C., 2011. Sediment redistribution due to a dense reservoir network in a large semi-arid Brazilian basin. *Hydrol. Sci. J.* 56 (2), 319–333. <https://doi.org/10.1080/02626667.2011.553616>.
- Linacre, E.T., 1993. Data-sparse estimation of lake evaporation using a simplified Penman equation. *Agric. Forest Meteorol.* 64 (3–4), 237–256. [https://doi.org/10.1016/0168-1923\(93\)90031-C](https://doi.org/10.1016/0168-1923(93)90031-C).
- Linacre, E.T., 1994. Estimating U.S. Class A pan evaporation from few climate data. *Water Int.* 19, 5–14.
- Lira, C.C.S., Medeiros, P.H.A., Lima Neto, I.E., 2020. Modelling the impact of sediment management on the trophic state of a tropical reservoir with high water storage variations. *Ann. Braz. Acad. Sci.* 92, 1–18. <https://doi.org/10.1590/0001-3765202020181169>.
- López, P.V., Alvarez, V.M., Elvira, B.G., Górriz, B.M., 2012. Determination of synthetic wind functions for estimating open water evaporation with Computational Fluid Dynamics. *Hydrol. Process* 26, 3945–3952.
- López Moreira M., G.A., Hinegk, L., Salvador, A., Zolezzi, G., Höller, F., Monte Domecq S., R.A., Bocci, M., Carrer, S., De Nat, L., Escrivá, J., Escrivá, C., Benítez, G.A., Ávalos, C.R., Peralta, I., Insaurralde, M., Merelles, F., Sekatchoff, J.M., Wehrle, A., Facetti-Masulli, J.F., Facetti, J.F., Toffolon, M., 2018. Eutrophication, research and management history of the Shallow Ypacaraí Lake (Paraguay). *Sustainability* 10 (7), 2426. <https://doi.org/10.3390/su10072426>.
- Majidi, M., Alizadeh, A., Farid, A., Vazifedoust, M., 2015. Estimating evaporation from lakes and reservoirs under limited data condition in a semi-arid region. *Water Resour. Manage.* 29, 3711–3733. <https://doi.org/10.1007/s11269-015-1025-8>.
- Mamede, G.L., Araújo, N.A.M., Schneider, C.M., de Araújo, J.C., Herrmann, H.J., 2012. Overspill avalanching in a dense reservoir network. *PNAS* 109 (19), 7191–7195. <https://doi.org/10.1073/pnas.1200398109/-DCSupplemental>.
- McGloin, R., McGowan, H., McJannet, D., Burn, S., 2014. Modelling sub-daily latent heat fluxes from a small reservoir. *J. Hydrol.* 519, 2301–2311. <https://doi.org/10.1016/j.jhydrol.2014.10.032>.
- McJannet, D.L., Webster, I.T., Cook, F.J., 2012. An area-dependent wind function for



- estimating open water evaporation using land-based meteorological data. *Environ. Modell. Software* 31, 76–83. <https://doi.org/10.1016/j.envsoft.2011.11.017>.
- Mcjannet, D.L., Hawdon, A., Niel, T.V., Boadle, D., Baker, B., Trefry, M., Rea, I., 2017. Measurements of evaporation from a mine void lake and testing of modelling approaches. *J. Hydrol.* 555, 631–647. <https://doi.org/10.1016/j.jhydrol.2017.10.064>.
- Mesquita, J.B.F., Pereira, S.P., Lima Neto, I.E., 2020. Urban drainage modeling and evaluation of bacteriological loads in the Vertente Marítima of Fortaleza, Ceará. *Sanitary Environ. Eng.* 25 (1), 205–216. <https://doi.org/10.1590/s1413-41522020189161>.
- Morton, F.I., 1983. Operational estimates of lake evaporation. *J. Hydrol.* 66 (1–4), 77–100. [https://doi.org/10.1016/0022-1694\(83\)90178-6](https://doi.org/10.1016/0022-1694(83)90178-6).
- Morton, F.I., 1986. A practical estimates of lake evaporation. *Am. Meteorol. Soc.* 25, 371–387.
- Moura, D.S., Lima Neto, I.E., Clemente, A., Oliveira, S., Pestana, C., Melo, M.A., Capelo-Neto, J.C., 2019. Modeling phosphorus exchange between bottom sediment and water in tropical semiarid reservoirs. *Chemosphere.* <https://doi.org/10.1016/j.chemosphere.2019.125686>.
- Oliveira, G.M., Leitão, M.M.V.B.R., Galvão, C.O., Leitão, T.J.V., 2005. Estimativa da Evaporação e Análise do Uso do Coeficiente (Kp) do Tanque “CLASSE A” nas Regiões do Cariri e Sertão da Paraíba. *Revista Brasileira de Recursos Hídricos* 10 (4), 73–83.
- Oroud, I.M., 1995. Effects of salinity upon evaporation from pans and Shallow Lakes near the Dead Sea. *Theor. Appl. Climatol.* 52 (3–4), 231–240.
- Pacheco, C.H.A., Lima Neto, I.E., 2017. Effect of artificial circulation on the removal kinetics of cyanobacteria in a hypereutrophic Shallow Lake. *J. Environ. Eng.* 143 (12). [https://doi.org/10.1061/\(ASCE\)EE.1943-7870.0001289](https://doi.org/10.1061/(ASCE)EE.1943-7870.0001289).
- Pereira, S.B., Pruski, F.F., Silva, D.D., Ramos, M.M., 2009. Evaporação líquida no lago de Sobradinho e impactos no escoamento devido à construção do reservatório. *Revista Brasileira de Engenharia Agrícola e Ambiental* 13 (3), 346–352.
- Persson, I., Jones, I.D., 2008. The effect of water colour on lake hydrodynamics: a modelling study. *Freshw. Biol.* 53 (12), 2345–2355. <https://doi.org/10.1111/j.1365-2427.2008.02049.x>.
- Peter, S.J., de Araújo, J.C., Araújo, N.A.M., Herrmann, H.J., 2014. Flood avalanches in a semiarid basin with a dense reservoir network. *J. Hydrol.* 512, 408–420. <https://doi.org/10.1016/j.jhydrol.2014.03.001>.
- Read, J.S., Rose, K.C., 2013. Physical responses of small temperate lakes to variation in dissolved organic carbon concentrations. *Limnol. Oceanogr.* 58 (3), 921–931.
- Rinke, K., Yeates, P., Rothhaupt, K., 2010. A simulation study of the feedback of phytoplankton on thermal structure via light extinction. *Freshw. Biol.* 55, 1674–1693. <https://doi.org/10.1111/j.1365-2427.2010.02401.x>.
- Riveros-Iregui, D.A., Lenters, J.D., Peake, C.S., Ong, J.B., Healey, N.C., Singh, V.P., Xu, A.N.D.C.-Y., 1997. Evaluation and generalization of 13 mass-transfer Equations for determining free water evaporation. *Hydrol. Process.* 11 (832), 311–323.
- Ryan, Patrick J., Stolzenbach, Keith D., 1972. *Environmental Heat Transfer, in Engineering Aspects of Heat Disposal from Power Generation.* R. M. Parson Laboratory for Water Resources and Hydrodynamics, Department of Civil Engineering, Massachusetts Institute of Technology, Cambridge, MA.
- Singh, V.P., Xu, C.-Y., 1997. Evaluation and generalization of 13 mass-transfer equations for determining free water evaporation. *Hydrol. Process.* 11 (3), 311–323. [https://doi.org/10.1002/\(SICI\)1099-1085\(19970315\)11:3<311::AID-HYP446>3.0.CO;2-Y](https://doi.org/10.1002/(SICI)1099-1085(19970315)11:3<311::AID-HYP446>3.0.CO;2-Y).
- Soares, L.M.V., Silva, T.F.G., Vinçon-Leite, B., Eleutério, J.C., Lima, L.C., Nascimento, N.O., 2019. Modelling drought impacts on the hydrodynamics of a tropical water supply reservoir. *Inland Waters* 9 (4), 1–16. <https://doi.org/10.1080/20442041.2019.1596015>.
- Spencer, J.W., 1971. Fourier series representation of the position of the sun. *Search* 2 (5), 172.
- Warnaka, K., Pochop, L., 1988. Analyses of equations for free water evaporation estimates. *Water Resour. Res.* 24 (7), 979–984.
- Watras, C.J., Morrison, K.A., Rubsam, J.L., 2016. Effect of DOC on evaporation from small Wisconsin lakes. *J. Hydrol.* 540, 162–175. <https://doi.org/10.1016/j.jhydrol.2016.06.002>.
- Wunderlich, W., 1972. *Heat and Mass Transfer between a Water Surface and the Atmosphere*, Rpt. No. 14, Rpt. Publication No. 0-6803. Water Resources Research Laboratory, Tennessee Valley Authority, Division of Water Control Planning, Engineering Laboratory, Norris, TN.
- Zhang, C., Brett, M.T., Brattebo, S.K., Welch, E.B., 2018. How well does the mechanistic water quality model CE-QUAL-W2 represent biogeochemical responses to climatic and hydrologic forcing? *Water Resour. Res.* 54 (9), 6609–6624. <https://doi.org/10.1029/2018WR022580>.
- Zhang, Q., Liu, H., 2014. Seasonal changes in physical processes controlling evaporation over inland water. *J. Geophys. Res.: Atmos.* 119 (16), 9779–9992. <https://doi.org/10.1002/2014JD021797>.
- Ziaie, R., Mohammadnezhad, B., Taheriyoun, M., Karimi, A., Amiri, S., 2019. Evaluation of thermal stratification and eutrophication in Zayandeh Roud Dam reservoir using two-dimensional CE-QUAL-W2 model. *J. Environ. Eng.* 145 (6), 05019001. [https://doi.org/10.1061/\(ASCE\)EE.1943-7870.0001529](https://doi.org/10.1061/(ASCE)EE.1943-7870.0001529).
- Zouabi-Aloui, B., Gueddari, M., 2014. Two-dimensional modelling of hydrodynamics and water quality of a stratified dam reservoir in the southern side of the Mediterranean Sea. *Environ. Earth Sci.* 72 (8), 3037–3051. <https://doi.org/10.1007/s12665-014-3210-0>.